6240 *Biochemistry* **2009,** *48,* 6240–6248
DOI: 10.1021/bi9000563

BIOCHEMISTRY
including biophysical chemistry & molecular biology
Article

Activation of HydA$^{\Delta EFG}$ Requires a Preformed [4Fe-4S] Cluster[†]

David W. Mulder,[‡] Danilo O. Ortillo,[§] David J. Gardenghi,[‡] Anatoli V. Naumov,[‡] Shane S. Ruebush,[‡] Robert K. Szilagyi,[‡] BoiHanh Huynh,[§] Joan B. Broderick,[‡] and John W. Peters*[,‡]

[‡]*Department of Chemistry and Biochemistry, Montana State University, Bozeman, Montana 59715, and* [§]*Department of Physics, Emory University, Atlanta, Georgia 30322*

Received January 14, 2009; Revised Manuscript Received April 23, 2009

ABSTRACT: The H-cluster is a complex bridged metal assembly at the active site of [FeFe]-hydrogenases that consists of a [4Fe-4S] subcluster bridged to a 2Fe-containing subcluster with unique nonprotein ligands, including carbon monoxide, cyanide, and a dithiolate ligand of unknown composition. Specific biosynthetic gene products (HydE, HydF, and HydG) responsible for the biosynthesis of the H-cluster and the maturation of active [FeFe]-hydrogenase have previously been identified and shown to be required for the heterologous expression of active [FeFe]-hydrogenase [Posewitz, M. C., et al. (2004) *J. Biol. Chem. 279*, 25711−25720]. The precise roles of the maturation proteins are unknown; the most likely possibility is that they are directed at the synthesis of the entire 6Fe-containing H-cluster, the 2Fe subcluster, or only the unique ligands of the 2Fe subcluster. The spectroscopic and biochemical characterization of HydA$^{\Delta EFG}$ (the [FeFe]-hydrogenase structural protein expressed in the absence of the maturation machinery) reported here indicates that a [4Fe-4S] cluster is incorporated into the H-cluster site. The purified protein in a representative preparation contains Fe (3.1 ± 0.5 Fe atoms per HydA$^{\Delta EFG}$) and S^{2-} (1.8 ± 0.5 S^{2-} atoms per HydA$^{\Delta EFG}$) and exhibits UV−visible spectroscopic features characteristic of iron−sulfur clusters, including a bleaching of the visible chromophore upon addition of dithionite. The reduced protein gave rise to an axial $S = {}^1/_2$ EPR signal (g = 2.04 and 1.91) characteristic of a reduced $[4Fe\text{-}4S]^{+}$ cluster. Mössbauer spectroscopic characterization of ^{57}Fe-enriched HydA$^{\Delta EFG}$ provided further evidence of the presence of a redox active $[4Fe\text{-}4S]^{2+/+}$ cluster. Iron K-edge EXAFS data provided yet further support for the presence of a [4Fe-4S] cluster in HydA$^{\Delta EFG}$. These spectroscopic studies were combined with in vitro activation studies that demonstrate that HydA$^{\Delta EFG}$ can be activated by the specific maturases only when a [4Fe-4S] cluster is present in the protein. In sum, this work supports a model in which the role of the maturation machinery is to synthesize and insert the 2Fe subcluster and/or its ligands and not the entire 6Fe-containing H-cluster bridged assembly.

The [NiFe]- and [FeFe]-hydrogenases are widely distributed in nature and efficiently catalyze the reversible oxidation of molecular hydrogen ($H_2 \leftrightarrow 2H^+ + 2e^-$). The [NiFe]-hydrogenases, present in archaea and bacteria, generally function to oxidize molecular H_2 and provide reducing equivalents for metabolic processes, while the [FeFe]-hydrogenases, present in bacteria and eukarya, function more broadly to catalyze both proton reduction and H_2 oxidation (*2*, *3*). Recently, there has been a growing interest in these metalloenzymes because of their inherent applicability in the development of renewable H_2-based energy technology.

The active sites for both [NiFe]- and [FeFe]-hydrogenases have been determined by X-ray crystallography and are united by the presence of π acceptor CO[1] and CN^- ligands, which are not common in biology. These diatomic ligands stabilize low-spin and low-valent oxidation states of the metal centers at the active sites. For the [NiFe]-hydrogenase, the active sites from a variety of different sulfate-reducing bacterial sources have been determined to consist of a Ni atom coordinated to an Fe atom via two thiolate ligands and a bridging oxygen species (*4*). The Ni atom is further coordinated by two cysteine ligands from the protein, while the Fe atom is coordinated to two terminal CN^- ligands and one terminal CO ligand. In comparison, the [FeFe]-hydrogenase active site contains a 6Fe-containing complex cluster termed the H-cluster, as determined for

[†]This work was supported by AFOSR Multidisciplinary University Research Initiative Award FA9550-05-01-0365 (J.W.P.), NASA Astrobiology Institute Funded Astrobiology Biogeocatalysis Research Center Grant NNA08C-N85A (J.W.P., J.B.B., and R.K.S.), National Institutes of Health Grant GM47295 (B.H.), and National Science Foundation Grant NSF0755676 (R.K.S.).

*To whom correspondence should be addressed. Phone: (406) 994-7211. Fax: (406) 994-7212. E-mail: john.peters@chemistry.montana.edu.

[1]Abbreviations: CO, carbon monoxide; CN^-, cyanide; Fe-S, iron−sulfur; HydA$^{\Delta EFG}$, HydA expressed in a genetic background devoid of HydE, HydF, and HydG; LB, Luria-Bertani; IPTG, isopropyl β-D-1-thiogalactopyranoside; PMSF, phenylmethanesulfonyl fluoride; DTT, dithiothreitol; DT, sodium dithionite; EPR, electron paramagnetic resonance; EXAFS, extended X-ray absorption fine structure analysis; SDS−PAGE, sodium dodecyl sulfate−polyacrylamide gel electrophoresis; EDTA, ethylenediaminetetraacetic acid; XAS, X-ray absorption spectroscopy; HydF*, HydF containing the ligand modified 2Fe subcluster.

 Published on Web 05/12/2009

Clostridium pasteurianum (CpI) (*5*, *6*) and *Desulfovibrio desulfuricans* (*7*, *8*). The H-cluster consists of a [4Fe-4S] subcluster coordinated to a 2Fe subcluster via a cysteine thiolate ligand. The two Fe centers in the 2Fe subcluster are bridged via a five-atom dithiolate ligand and a CO ligand. The chemical composition of the dithiolate ligand has not yet been determined unambiguously and has been proposed to be dithiomethylether (*6*), propane dithiolate (*7*), or dithiomethylamine (*8*). In addition, both Fe centers contain terminal CO and CN^- ligands. For the presumed oxidized state of CpI, a water molecule is present at the distal Fe center in the proximity of the [4Fe-4S] subcluster.

Biosynthesis and maturation of the [NiFe]-hydrogenases have been thoroughly studied, including identification of at least six gene products involved in formation of active [NiFe]-hydrogenases and the interactions between gene products during maturation. The metabolic source of diatomic CN^- ligands has been identified to be carbamoyl phosphate (*9*), whereas the metabolic source for the CO ligand is still in question. In contrast, relatively little is known concerning the biosynthesis and maturation of [FeFe]-hydrogenases. By analysis of several mutant strains of *Chlamydomonas reinhardtii* that are unable to produce hydrogen, the genes *hydEF* and *hydG* were discovered to be required for maturation of [FeFe]-hydrogenases (*1*). Subsequent expression studies revealed that formation of an active [FeFe]-hydrogenase was achieved only when HydA was heterologously expressed in a background of coexpressed gene products HydEF and HydG in *Escherichia coli* (*1*). In most organisms, *hydEF* exists as two separate genes, *hydE* and *hydF* (*1*), and it has been shown that the coexpression in *E. coli* of HydE, HydF, and HydG from *Clostridium acetobutylicum* with the [FeFe]-hydrogenase structural gene product from various algal and bacterial sources is sufficient to effect expression of active [FeFe]-hydrogenase (*10*). Deduced amino acid sequence analysis of HydE, HydF, and HydG gene products reveals HydE and HydG to be radical-SAM Fe-S enzymes as they both have the C-X_3-C-X_2-C radical-SAM signature motif and HydF to be a GTPase (*1*, *9*). Also, preliminary biochemical characterization of HydE and HydG has revealed associated SAM cleavage activity (*11*). In addition, it has been shown that upon reconstitution HydF binds an Fe-S cluster and exhibits GTPase activity (*12*).

The involvement of HydE, HydF, and HydG maturation enzymes in the biosynthesis of the H-cluster was further elaborated when it was shown that HydA, expressed in a genetic background devoid of HydE, HydF, and HydG ($HydA^{\Delta EFG}$), is a stable protein capable of being activated in vitro by the aforementioned proteins (*13*). It was also determined that HydF behaves as a scaffold protein in which an H-cluster precursor is assembled and can be subsequently transferred to $HydA^{\Delta EFG}$, resulting in the formation of an active [FeFe]-hydrogenase (*14*). Both in vitro activation studies imply that cluster biosynthesis does not take place on the structural protein ($HydA^{\Delta EFG}$) and that a chemical precursor to the H-cluster is synthesized in the absence of $HydA^{\Delta EFG}$ that upon transfer to $HydA^{\Delta EFG}$ results in its activation. Although no chemical precursors or intermediates to the H-cluster have yet been characterized or even identified, it can be hypothesized that HydE, HydF, and HydG are directed toward the synthesis of (1) the entire 6Fe-containing H-cluster, (2) the 2Fe subcluster of the H-cluster, or (3) the biologically unique ligands of the 2Fe subcluster of the H-cluster. The characterization of $HydA^{\Delta EFG}$ provides a critical link in our understanding of this fascinating process by defining the substrate for the Hyd maturation proteins.

In this study, we present spectroscopic and biochemical characterizations of $HydA^{\Delta EFG}$ from *C. reinhardtii* to provide insights into the [FeFe]-hydrogenase maturation and H-cluster biosynthesis. HydA from the eukaryotic green algae *C. reinhardtii* contains only the H-cluster binding domains and represents the simplest [FeFe]-hydrogenase known. Unlike [FeFe]-hydrogenases from *Cl. pasteurianum* and *D. desulfuricans*, the [FeFe]-hydrogenases from eukaryotic green algae do not contain additional accessory Fe-S clusters with plant-type ferredoxin domains that would complicate spectroscopic characterization of the Fe-S clusters present at the active site (*15*−*17*). Our characterization of $HydA^{\Delta EFG}$ from *C. reinhardtii* indicates that a [4Fe-4S] cluster is present in $HydA^{\Delta EFG}$ and is required for in vitro activation by the HydE, HydF, and HydG maturation enzymes. Accordingly, it follows that the aforementioned maturation enzymes are not directed at the synthesis of the entire 6Fe-containing H-cluster.

EXPERIMENTAL PROCEDURES

Cloning and Cell Growth Conditions. $HydA^{\Delta EFG}$ from *C. reinhardtii* was cloned into a pET Duet vector as described previously (*10*) and modified for the presence of an N-terminal six-histidine tag. $HydA^{\Delta EFG}$ from *C. reinhardtii* was expressed in *E. coli* BL21(DE3) cells and cultivated in either 2 L flasks with a 1 L medium volume or a 10 L benchtop fermentor (New Brunswick) containing modified MOPS minimal medium (*18*) supplemented with 5.5% glucose and 150 μg/mL ampicillin. Either 5 or 50 mL overnight cultures of BL21(DE3) cells were used to inoculate 1 or 10 L cultures, respectively. Later, cell expressions were cultivated in LB medium buffered with 50 mM phosphate (pH 7.6), supplemented with 5.5% glucose and 150 μg/mL ampicillin. The cells were grown at 37 °C with vigorous shaking (flasks) and agitation and aeration (fermentor, 250 rpm, 3 L/min) to an optical density of 0.5 (measured at 600 nm with a visible spectrophotometer from Thermo Spectronic) and induced by addition of IPTG to a final concentration of 1 mM. $(NH_4)_2Fe(SO_4)_2 \cdot 6H_2O$ (191 μM) was also added at induction. Induction was allowed to proceed aerobically for 2 h at 37 °C followed by 16 h at 4 °C under nitrogen purge with additional supplemented $(NH_4)_2Fe(SO_4)_2 \cdot 6H_2O$ (191 μM). The cells were harvested anaerobically (8000 rpm and, 4 °C), washed with buffer A [50 mM HEPES (pH 7.6), 150 mM NaCl, and 1 mM DTT] in an anaerobic Coy chamber (Coy Laboratories), and stored at −80 °C.

$HydA^{\Delta EFG}$ Purification. Cell-free extracts were prepared by resuspending the cells (described above) in degassed anaerobic buffer B [5 mL of buffer/g of cells, 50 mM HEPES (pH 7.6), 50 mM NaCl, 5% (w/v) glycerol, 1% (w/v) Triton X-100, 10 mM $MgCl_2$, 1 mM PMSF, 1 mM DTT, and trace quantities of lysozyme and DNAase] and placing the suspension in a pressure cell bomb (1000 psi nitrogen pressure, 1 h) followed by centrifugation of the lysate (36,000 × G for 45 min). $HydA^{\Delta EFG}$ was purified from the cell lysate by anion exchange chromatography on Q-Sepharose resin (GE Healthcare) followed by *His*-tag affinity chromatography to a Co^{2+} resin (Talon resin; Clontech); all purification steps were done anaerobically using thoroughly degassed buffers under positive nitrogen pressure. Cell lysates were loaded onto a 100 mL Q-Sepharose column previously equilibrated in buffer C [50 mM HEPES (pH 7.6), 20% glycerol, and 1 mM DT]. The column was washed with buffer C supplemented with 100 mM NaCl, and $HydA^{\Delta EFG}$ was eluted

with buffer C in arrangement with a NaCl gradient up to a final concentration of 1 M while the absorbance at 405 nm was monitored. HydA$^{\Delta EFG}$ protein-containing fractions were golden-brown in color, consistent with the presence of Fe-S clusters. These fractions were loaded onto a 25 mL Co^{2+} affinity column. The column, equilibrated with buffer D [50 mM HEPES (pH 7.0), 300 mM NaCl, 20% glycerol, 0.5 mM DT, and 5 mM βME], was washed with buffer D supplemented with 10 mM imidazole, and HydA$^{\Delta EFG}$ was eluted using an imidazole gradient up to 100 mM in buffer D while the absorbance at 405 nm was monitored. The golden-brown protein-containing fractions were concentrated using an Amicon concentration cell under positive argon pressure with a 30 kDa cutoff membrane filter. The protein was desalted in a Coy anaerobic chamber using a Sephadex 2 mL G-25 column (GE Healthcare) equilibrated with buffer C and stored under liquid nitrogen. Overall, six different HydA$^{\Delta EFG}$ protein preparations were used. For later preparations, it was determined that the quality of the spectroscopic data collected could be improved by selectively saving HydA$^{\Delta EFG}$ fractions with the highest 405 nm to 280 nm absorbance ratios as measured after elution from the Q-Sepharose and Co^{2+} *His*-tag affinity columns.

Assays. Protein concentrations were determined using the Bradford assay (*19*) with bovine serum albumin (Sigma) as the standard. The specific hydrogenase activity of the purified HydA$^{\Delta EFG}$ was measured using gas chromatography upon maximum in vitro activation with cell lysates containing maturation proteins HydE, HydF, and HydG from *Cl. acetobutylicum* as described by McGlynn et al. (*13*). In the assays, dithionite (20 mM) was used as the reducing agent, methyl viologen (10 mM) was used as the electron carrier, and HydE, HydF, and HydG cell extracts from *Cl. acetobutylicum* were used to activate HydA$^{\Delta EFG}$. The iron content of HydA$^{\Delta EFG}$ was determined using a procedure described by Fish (*20*), which uses ferrozine under reductive conditions after digestion of the protein in 4.5% (w/v) $KMnO_4$ and 1.2 N HCl. Iron standards were prepared by dilution of a commercial Fe AA standard (Ricca Chemical Co.). Sulfide assays were conducted according to a procedure described by Beinert (*21*) and Broderick (*22*), and sulfide standards were prepared from $Na_2S \cdot 9H_2O$.

Electronic Absorption Spectroscopy. For UV−visible spectroscopic experiments, samples were prepared inside an anaerobic Coy chamber and transferred to anaerobic 1 mL cuvettes (NSG Precision Cells, Inc.). UV−visible spectra were recorded at room temperature with a Cary 300 (Varian) spectrophotometer. Reduced samples were prepared by adding 2 mM DT.

EPR Spectroscopy. Low-temperature X-band EPR spectra were recorded using a Bruker ESP300E spectrometer equipped with a liquid helium cryostat and temperature controller from Oxford Instruments. Typical EPR parameters were as follows: sample temperature, 12 K; microwave frequency, 9.36 GHz; attenuation, 20.4 dB; and microwave power, 1.85 mW. Sample concentrations varied between 128 and 512 μM. Reduced samples were prepared by adding 2 mM DT, and oxidized samples were prepared by titrating in increasing concentrations of ferricyanide (2−11 mM). The spin concentration was determined by double integration of the sample spectra using $CuSO_4$ (0.20 mM) and EDTA (2.0 mM) as the standard measured under identical conditions. Basic analysis of the collected spectra was conducted using the computer software program SpinCount (M. Hendrich, Carnegie Mellon University, Pittsburgh, PA).

Mössbauer Spectroscopy. ^{57}Fe was purchased from Cambridge Isotope Laboratories, Inc., and dissolved in hot concentrated hydrochloric acid. The pH was adjusted with NaOH. HydA$^{\Delta EFG}$ as-isolated ^{57}Fe samples were prepared from 10 L cultures using the defined minimal medium (*18*) described above with ^{57}Fe substituted at the same molar concentrations for ^{56}Fe. ^{57}Fe (191 μM) was also added at induction with IPTG. Protein samples (500−800 μM) were loaded into 450 μL cups and stored under liquid nitrogen. Mössbauer spectra were recorded on a Mössbauer spectrometer equipped with a Janis 8DT variable-temperature cryostat and operated at a constant acceleration mode in transmission geometry. The zero velocity refers to the centroid of a room-temperature spectrum of a metallic iron foil. Analysis of the spectra was performed with WMOSS (WEB Research).

Fe K-Edge X-ray Absorption Spectroscopy. HydA$^{\Delta EFG}$ samples (1.9 mM) were prepared from the HydA$^{\Delta EFG}$ protein isolated as described above. The EXAFS cells (Delrin) sealed with thin Fe-free Kapton tape were loaded with ~100 μL of sample. Fe K-edge X-ray absorption spectroscopic (XAS) measurements were conducted at beamline 7-3 (BL7-3) of the Stanford Synchrotron Radiation Lightsource (SSRL) under storage ring (SPEAR3) conditions with an energy of 3 GeV and a current of 100−80 mA on two different occasions. BL7-3 is a 20-pole, 2 T Wiggler beamline equipped with a Si(220) downward reflecting, double-crystal monochromator. Data were collected in the energy range from 6785 eV to k = 17 Å^{-1} above the Fe K-edge using an unfocused beam. The frozen solution samples were mounted under liquid nitrogen and measured in a liquid He cryostat at ~11 K. The beamline parameters were optimized at 8000 eV. The Fe Kα fluorescence signal was collected using a 30-element Ge array detector and with a Soller slit and Z-1 (Mn) filter. The energy windowing of the detector was carefully done to minimize the fluorescence signal due to scattering and other non-Fe Kα emission sources.

ATHENA (*23*), a graphical-user interface to *IFEFFIT* (*23*), was used for averaging and background subtraction. The data were calibrated to the first rising-edge inflection point of the XAS spectra that was assigned to 7111.2 eV of an iron foil. The data are averages of at least five scans before normalization or background subtraction. *ATHENA* and *AUTOBK* were used to spline the postedge region and to obtain the EXAFS with an R_{bkg} of 1.

ARTEMIS (*23*), *ATOMS* (*23*), and *FEFF* (*24*) were used to model and fit the data and calculate Fe···Fe and Fe-S scattering paths, respectively. The structural models used in scattering calculations were derived from combination of average Fe···Fe and Fe−S distances of reduced and oxidized [4Fe-4S] model compounds (*25*). Due to the presence of various Fe environments which lead to various reasonable fits [defined as R(fit) < 10^{-3}], we used the composition of Fe-S clusters in the EXAFS fits as constraints from corresponding Mössbauer measurements.

Reconstitution of Iron−Sulfur Clusters in HydA$^{\Delta EFG}$. HydA was subjected to reconstitution conditions following the general procedures described for biotin synthase (*26*). The protein (10 μM) was incubated with $FeCl_3$ (100 μM), Na_2S (100 μM), and DTT (1 mM) in buffer E [50 mM HEPES (pH 7.0), 300 mM NaCl, and 20% glycerol] for 2−3 h with constant stirring in an anaerobic Coy chamber. Visually, the color of the diluted protein solution was observed to change to golden brown. All reagents were added sequentially, and following reconstitution, excess ions were removed using a G-25 Sephadex column.

The resulting reconstituted HydA$^{\Delta EFG}$ was assayed for hydrogenase activity by in vitro activation with HydE, HydF, and HydG from *Cl. acetobutylicum*, and iron content was also analyzed as described earlier.

Preparation of Apo-HydA$^{\Delta EFG}$ and Reconstitution. Apo-HydA$^{\Delta EFG}$ from *C. reinhardtii* was prepared by stripping out all Fe-S clusters using EDTA as an Fe chelator. HydA$^{\Delta EFG}$ from *C. reinhardtii* was incubated aerobically with EDTA (100 mM) for 1 h in buffer E. Fe-S cluster chelation was monitored visually, and within 1 h, the golden-brown protein solution turned colorless. The resulting apoprotein was made anaerobic by degassing it under vacuum with sequential nitrogen purge and incubation with 5 mM DTT. Excess EDTA was removed with a G-25 Sephadex column, and verification that all Fe was stripped from the protein was achieved by Fe analysis. Apo-HydA$^{\Delta EFG}$ from *C. reinhardtii* was reconstituted by incubating the protein (1 μM) with a large excess of $FeCl_3$, Na_2S, and DTT (1 mM) in buffer E for 2−3 h. Residual $FeCl_3$ and Na_2S were removed with a G-25 Sephadex column, and the protein was concentrated with a 30 kDa Centricon centrifugal filter device (Millipore). The colorimetric iron assay was used to monitor addition of Fe. The hydrogenase activities of the different HydA$^{\Delta EFG}$ forms (HydA$^{\Delta EFG}$, apo-HydA$^{\Delta EFG}$, and reconstituted apo-HydA$^{\Delta EFG}$) were determined following activation with the HydE, HydF, and HydG maturation enzymes.

RESULTS AND DISCUSSION

HydA$^{\Delta EFG}$ Binds a [4Fe-4S] Cluster. Anaerobic purification of heterologously expressed *C. reinhardtii* HydA$^{\Delta EFG}$ [49 kDa (Figure 1A)] in *E. coli* gives a stable protein that is capable of being activated in vitro by *Cl. acetobutylicum* extracts containing HydE, HydF, and HydG. Specific activities of the six separate HydA$^{\Delta EFG}$ protein purifications after in vitro activation with HydE, HydF, and HydG enzymes ranged from 10 to 38 μmol of H_2 min^{-1} (mg of HydA$^{\Delta EFG}$)$^{-1}$. For in vivo coexpression of HydA from *C. reinhardtii* with the maturation genes from *Cl. acetobutylicum* in *E. coli*, H_2 evolution activity was previously reported to be 150 μmol of H_2 min^{-1} mg^{-1} (*10*). The difference in activity between in vitro and in vivo expression systems is likely attributed to the low occupancy of H-cluster activating precursors assembled by HydE, HydF, and HydG, as well as the heterogeneity of the maturation system (*14*). It was evident that HydA$^{\Delta EFG}$ binds Fe-S clusters as observed by the dark brown color of the protein solution following purification as well as Fe (3.1 ± 0.5 Fe atoms/HydA$^{\Delta EFG}$) and S^{2-} (1.8 ± 0.5 S^{2-} atoms/HydA$^{\Delta EFG}$) analyses. It is important to note that the amount of Fe and S^{2-} bound per HydA$^{\Delta EFG}$ varied slightly between different purifications, suggesting that the Fe-S cluster present may be slightly labile during purification. The UV−visible absorbance spectrum shows a broad shoulder centered near 405 nm that upon reduction with DT decreases in intensity (Figure 1B). These absorbance features are consistent with the presence of Fe-S clusters in HydA$^{\Delta EFG}$. This was further confirmed by the low-temperature X-band EPR spectrum of reduced HydA$^{\Delta EFG}$ which revealed an axial $S = {}^1/_2$ signal (g = 2.04 and 1.91) characteristic of a reduced $[4Fe\text{-}4S]^+$ cluster (Figure 2) (*27*). Also, a slight shoulder was observed at g = 2.04; however, the appearance of this feature varied between different protein preparations and could be minimized when the protein was further purified on the basis of collection of protein fractions with maximal 405 nm to 280 nm absorbance. The temperature and power dependence of the axial $S = {}^1/_2$ signal showed a maximum intensity around temperatures of 10 K and diminished significantly at temperatures greater than 30 K at a power of 2 mW (Supporting Information). The signal was no longer

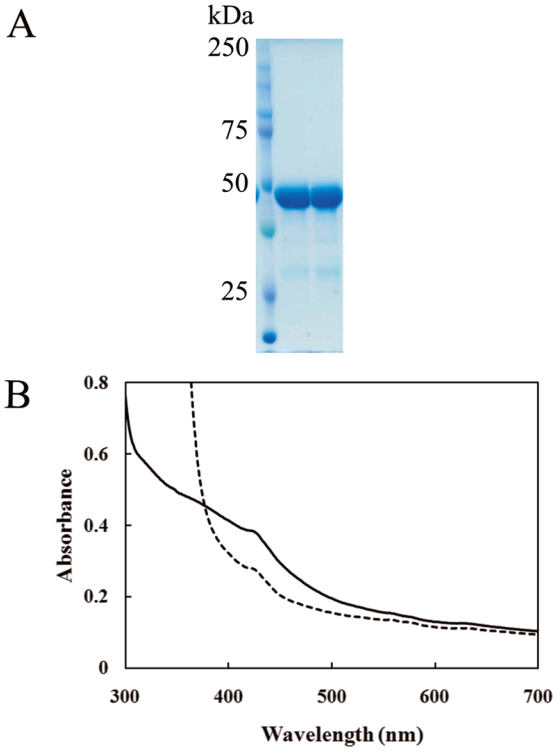

FIGURE 1: (A) SDS−PAGE gel (10%) showing purification of HydA$^{\Delta EFG}$ from *C. reinhardtii* following elution from the Co^{2+} *His*-tag affinity column. The left lane shows the protein marker standards, and the right lanes show the pure HydA$^{\Delta EFG}$ from *C. reinhardtii* at 49 kDa. (B) UV−visible spectra of HydA$^{\Delta EFG}$ as isolated (—) and HydA$^{\Delta EFG}$ reduced with 2 mM DT (--). The feature centered at 400 nm is characteristic of Fe-S cluster LMCT bonds.

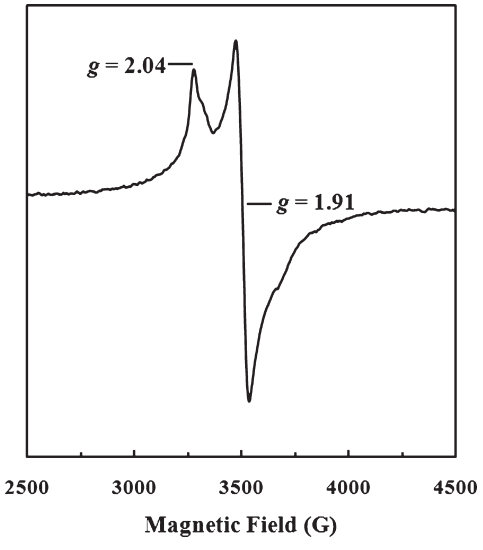

FIGURE 2: EPR spectrum of reduced HydA$^{\Delta EFG}$. Parameters for EPR measurement were as follows: sample temperature, 12 K; microwave frequency, 9.36 GHz; attenuation, 20.4 dB; microwave power, 1.85 mW; receiver gain, 2.0×10^4. The reduced sample was prepared by adding 2 mM DT to as-isolated HydA$^{\Delta EFG}$ (235 μM). Upon oxidation of HydA$^{\Delta EFG}$ with ferricyanide, the [4Fe-4S] cluster signal is no longer observed.

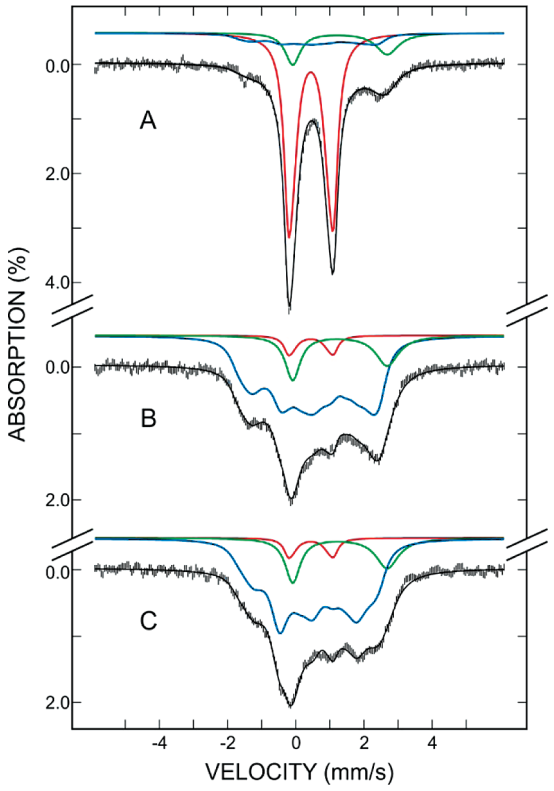

FIGURE 3: Mössbauer spectra of as-purified (A) and dithionite-reduced (B and C) HydA$^{\Delta EFG}$. The spectra (hatched marks) were recorded at 4.2 K in a magnetic field of 50 mT applied parallel (A and B) and perpendicular (C) to the γ radiation. The solid lines plotted above the data are simulated spectra for the [4Fe-4S]$^{2+}$ cluster (red), [4Fe-4S]$^{+}$ cluster (blue), and Fe^{II} impurities (green), normalized to the following percent absorptions: (A) 70% [4Fe-4S]$^{2+}$, 15% [4Fe-4S]$^{+}$, and 15% Fe^{II} and (B and C) 6% [4Fe-4S]$^{2+}$, 76% [4Fe-4S]$^{+}$, and 18% Fe^{II}. The black lines overlaid with the experimental spectra are composite spectra. Parameters used for the simulations are given in the text (for the [4Fe-4S]$^{2+}$ and Fe^{II} impurities) and in the Supporting Information (for the [4Fe-4S]$^{+}$ cluster).

observed above temperatures of 40 K and also did not saturate with an increase in microwave power. These temperature and power signal characteristics are typical for the presence of a [4Fe-4S]$^{+}$ cluster (*28*). Spin quantification of the signal, using $CuSO_4$ (0.20 mM) with EDTA (2.0 mM) as a standard, gave 0.17 spin/Fe atom. Upon oxidation of HydA$^{\Delta EFG}$ with ferricyanide, the [4Fe-4S]$^{+}$ cluster signal disappeared and no EPR signal was observed (data not shown).

Mössbauer Spectroscopic Characterization of HydA$^{\Delta EFG}$. Figure 3 shows the Mössbauer spectra of the ^{57}Fe-enriched HydA in its as-purified (A) and dithionite-reduced (B and C) forms. The spectra were recorded at 4.2 K in a magnetic field of 50 mT applied parallel (A and B) and perpendicular (C) to the γ radiation. Analysis of the data indicates that all three spectra are composed of three subspectral components: a central quadrupole doublet (solid red lines in Figure 3), a magnetically split spectrum (blue lines), and an outer quadrupole doublet with broad and asymmetric absorption lines (green lines). The central quadrupole doublet is attributed to a [4Fe-4S]$^{2+}$ cluster and can be simulated as a superposition of two unresolved equal-intensity quadrupole doublets representing the two mixed-valence Fe^{II}-Fe^{III} pairs within the cluster. The parameters obtained for the two unresolved doublets [$\Delta E_Q(1)$ = 1.34 mm/s, $\delta(1)$ = 0.45 mm/s, and $\Gamma(1)$ (line width) = 0.30 mm/s; $\Delta E_Q(2)$ = 1.05 mm/s, $\delta(2)$ = 0.44 mm/s, and $\Gamma(2)$ = 0.43 mm/s] are typical for [4Fe-4S]$^{2+}$ clusters (*29*, *30*). The magnetically split spectral component exhibits an intensity pattern that depends on the direction of the applied field (blue lines in panels B and C), indicating that it originates from an EPR active Fe center. As reported above, reduced HydA displays an $S = {}^1/_2$ EPR signal that can be assigned to a [4Fe-4S]$^{+}$ cluster. The magnetic Mössbauer spectral component is therefore attributed to this $S = {}^1/_2$ Fe cluster. Consistent with the [4Fe-4S]$^{+}$ assignment, initial analysis of this spectral component indicates that it may be simulated as a superposition of two spectral components arising from the Fe^{II}Fe^{II} and Fe^{II}Fe^{III} pairs of a [4Fe-4S]$^{+}$ cluster (see the Supporting Information) (*29*, *30*). On the basis of the parameters obtained for the outer quadrupole doublet [ΔE_Q = 2.77 mm/s, δ = 1.30 mm/s, Γ(left) = 0.53 mm/s, and Γ(right) = 0.80 mm/s], this component is attributed to non-cysteine-coordinated extraneous Fe^{II} impurities, which may be generated via cluster degradation.

Decomposition of the Mössbauer spectra into the above-described spectral components shows that in the as-purified HydA$^{\Delta EFG}$ sample (see Figure 3A) the majority (70%) of the Fe is present in the oxidized [4Fe-4S]$^{2+}$ form while a small percentage (15%) is in the reduced [4Fe-4S]$^{+}$ form. The remaining Fe (15%) is present as Fe^{II} impurities. Upon reduction (see Figure 3B,C), a substantial amount of the [4Fe-4S]$^{2+}$ clusters are reduced to [4Fe-4S]$^{+}$ clusters, resulting in a decrease in the Mössbauer absorption of the [4Fe-4S]$^{2+}$ cluster from 70 to 6% and an increase in the [4Fe-4S]$^{+}$ absorption to 76%. That of the Fe^{II} impurities also increases slightly to 18%, suggesting that the [4Fe-4S] cluster in HydA$^{\Delta EFG}$ is slightly unstable under dithionite reducing conditions. Thus, the Mössbauer data unambiguously show that the as-purified HydA$^{\Delta EFG}$ contains predominantly [4Fe-4S] clusters. No other types of Fe-S clusters are detected. The observation that the [4Fe-4S]$^{2+}$ cluster in HydA$^{\Delta EFG}$ can be reduced by dithionite to the [4Fe-4S]$^{+}$ state establishes further that HydA$^{\Delta EFG}$ contains a redox active [4Fe-4S]$^{2+/+}$ cluster. Taking into consideration the Fe and protein content (1.9 Fe atoms/HydA$^{\Delta EFG}$) determined for the as-purified ^{57}Fe-enriched HydA$^{\Delta EFG}$ and the total percent absorption of the [4Fe-4S] cluster detected by the Mössbauer measurement (85%), we find a stoichiometry of 0.4 [4Fe-4S] cluster/HydA$^{\Delta EFG}$ for the as-purified HydA$^{\Delta EFG}$.

Fe K-Edge X-ray Absorption Spectroscopic Characterization of HydA$^{\Delta EFG}$. The Fourier transforms of EXAFS (FT-EXAFS) for the as-isolated HydA sample (black trace) and with a representative fit (red trace) are shown in Figure 4. The fitting parameters are summarized in Table 1. Among numerous reasonable fits with R(fit) values of 10^{-4}, Table 1 and Figure 4 report the one that was obtained using the Mössbauer results (see above) as constraints for the amount and distribution of various Fe sites. The initial parameters of the fit were set to represent the 70% oxidized and 15% reduced protein-embedded [4Fe-4S] cluster content. The average Fe$\cdots$Fe, Fe$-$S^t, and Fe$-$S^s distances in synthetic [4Fe-4S] complexes are 2.74 $\pm$ 0.01, 2.25 $\pm$ 0.01, and 2.27 $\pm$ 0.03 Å, respectively (*25*). The protein-bound counterparts of Fe-S distances tend to be ~0.02 Å longer due to dipole and hydrogen bonding interactions involving the sulfides and thiolate sulfurs, which reduces the nucleophilicity of the sulfur atoms and thus the covalency of the sulfur$-$iron bonds. These differences between the synthetic model and protein-bound Fe-S clusters can be observed by EXAFS as demonstrated by a series of FT-EXAFS analyses of Fe-S clusters (*31*$-$*33*). Using the initial distances with standard deviations as initial

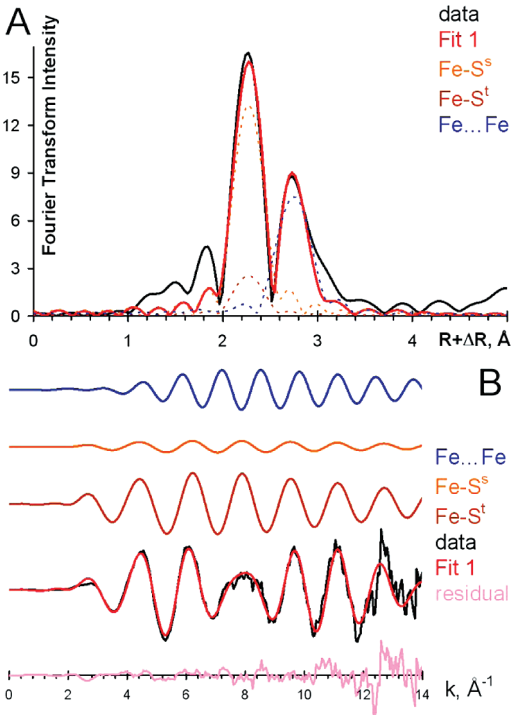

FIGURE 4: FT-EXAFS plot (A) and individual EXAFS contributions (B) for the as-isolated HydA$^{\Delta EFG}$ sample with a representative fit containing Fe···Fe, Fe−S(sulfide), and Fe−S(thiolate) scattering paths.

Table 1: Representative Fitting Parameters for the As-Isolated HydA$^{\Delta EFG}$ Sample Using the Fe-S Composition from Mössbauer Measurements

scatterer	parameter[a]	fitted value
Fe−S^s	r (Å)	2.27
	N	3
	A	0.80
	σ^2 (Å^2)	0.003
Fe−S^t	r (Å)	2.27
	N	1
	A	0.46
	σ^2 (Å^2)	0.003
Fe···Fe	r (Å)	2.72
	N	3
	A	0.44
	σ^2 (Å^2)	0.003
	R(fit)	7.65 10^{-4}
	E_0 (eV)	0.790

[a] r, scattering path; N, coordination number; A, scattering path amplitude; σ^2, Debye−Waller factor as a measure of thermal displacement and disorder. k^3-weighted data fit in the k range of 1−14 Å^{-1}; FT-EXAFS window range fitted 1.5−3.3 Å.

Debye−Waller factors of 2.74 ± 0.005, 2.24 ± 0.003, and 2.28 ± 0.003 Å for Fe···Fe, Fe−S^t, and Fe−S^s scattering paths, respectively, we obtained a reasonable fit that is shown in Figure 4. To prevent negative Debye−Waller factors (σ^2) and large deviations of the edge positions (E_0), we obtained the final fit by linking all the σ^2 and E_0 values while allowing the individual path lengths and their amplitudes to vary. The parameters in Table 1 fit acceptably well with the bulk of the experimental data (black trace), but a poor fit was found at the shorter distances. The residual FT-EXAFS intensity at these distances is consistent with the presence of ~15% free iron that is likely partially solvated and/or coordinated with low-Z atoms, such as O and N from protein residues as suggested by Mössbauer results. The peak at around 1.9 ± 0.1 Å can be reasonably well fitted with an Fe center surrounded by six low-Z (O and N) scatterers in 15% abundance. The relatively short Fe−O distance of 1.9 Å is indicative of the presence of negatively charged O or N ligands for the Fe^{II} impurities (see above). The fit components and parameters for the latter are given as Supporting Information. For both FT-EXAFS fits, the resulting Fe···Fe (2.71−2.72 Å) and Fe−S (2.27 Å) distances are highly similar to those observed for the oxidized and reduced [4Fe-4S] cluster in Av2 (2.72 and 2.73 Å, and 2.27 and 2.29 Å, respectively) (*33*) and thus further support the presence of the [4Fe-4S] cluster in HydA$^{\Delta EFG}$.

Reconstitution of the [4Fe-4S] Cluster in HydA$^{\Delta EFG}$. It was previously reported that HydA$^{\Delta EFG}$ can be activated by cell extracts containing the maturation enzymes HydE, HydF, and HydG (*13*). This observation, coupled with our evidence described above for a [4Fe-4S] cluster in HydA$^{\Delta EFG}$, suggests that the [4Fe-4S] form of HydA$^{\Delta EFG}$ is the substrate for assembly of the H-cluster by HydE, HydF, and HydG and further that the [4Fe-4S] cluster present in HydA$^{\Delta EFG}$ becomes part of the H-cluster upon activation. To further explore the requirement for a preformed [4Fe-4S] cluster in HydA$^{\Delta EFG}$ during activation with HydE, HydF, and HydG, HydA$^{\Delta EFG}$ was chemically reconstituted with $FeCl_3$ and Na_2S. Fe analysis of the reconstituted HydA$^{\Delta EFG}$ gave 4.0 ± 0.1 Fe/HydA$^{\Delta EFG}$, and the EPR spectrum of reconstituted reduced HydA$^{\Delta EFG}$ indicates the presence of a [4Fe-4S] cluster, with an axial $S = {}^1/_2$ EPR signal (g = 2.04 and 1.91) essentially identical to that of the as-isolated enzyme. In vitro activation of the reconstituted HydA$^{\Delta EFG}$ with HydE, HydF, and HydG gave hydrogenase activity [31.5 ± 0.5 μmol of H_2 min^{-1} (mg of HydA$^{\Delta EFG}$)$^{-1}$] approximately 2-fold greater than that of the as-isolated HydA$^{\Delta EFG}$ activated with HydE, HydF, and HydG [17.1 ± 2.4 μmol of H_2 min^{-1} (mg of HydA$^{\Delta EFG}$)$^{-1}$]. These observations provide additional evidence that the [4Fe-4S] form of HydA is the substrate for H-cluster assembly by HydE, HydF, and HydG, as increasing the [4Fe-4S] content improves the ability to activate HydA$^{\Delta EFG}$. In addition, the reconstitution results are consistent with our previous suggestion that the [4Fe-4S] cluster in HydA$^{\Delta EFG}$ is labile during purification and is subsequently repopulated or repaired during reconstitution. In contrast, if the [4Fe-4S] cluster present in HydA$^{\Delta EFG}$ was not required for activation by HydE, HydF, and HydG, it is likely that reconstitution would inhibit in vitro activation by generating a cluster at the H-cluster site that would prevent activation by the maturation enzymes.

Metal Chelation and Reconstitution. To further explore the hypothesis that the [4Fe-4S] cluster present in HydA$^{\Delta EFG}$ is required for in vitro activation with HydE, HydF, and HydG, apo-HydA$^{\Delta EFG}$ was prepared and then subsequently reconstituted with $FeCl_3$ and Na_2S; both apo and reconstituted samples were subjected to in vitro activation by HydE, HydF, and HydG (Figure 5). The apo sample was found to contain zero Fe atoms per HydA$^{\Delta EFG}$, and upon in vitro activation with HydE, HydF, and HydG maturation enzymes, the apo-HydA$^{\Delta EFG}$ protein exhibited no hydrogenase activity. Following chemical reconstitution of apo-HydA$^{\Delta EFG}$ with $FeCl_3$ and Na_2S, the protein contained 4.0 ± 0.1 Fe atoms/HydA$^{\Delta EFG}$ and had an EPR spectrum essentially identical to that of the as-isolated enzyme. Subsequent in vitro activation of the reconstituted enzyme with HydE, HydF, and HydG produced hydrogenase activity

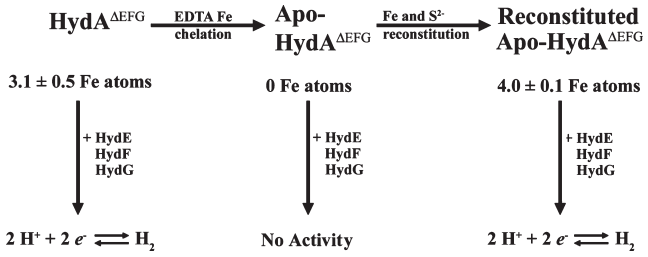

FIGURE 5: (A) Flow scheme outlining Fe content and hydrogenase activity during preparation of apo-HydA$^{\Delta EFG}$ by stripping out all existing Fe−S clusters in HydA$^{\Delta EFG}$ and the ensuing reconstitution of apo-HydA$^{\Delta EFG}$. Apo-HydA$^{\Delta EFG}$ shows no hydrogenase activity following in vitro activation. Reconstituted apo-HydA$^{\Delta EFG}$ displayed 90% of initial hydrogenase activity (compared to as-isolated HydA$^{\Delta EFG}$) upon in vitro activation with maturases. Also, Fe analysis of the reconstituted apo-HydA$^{\Delta EFG}$ gave 4.0 ± 0.1 Fe atoms/protein.

at a level of 90% of that of as-isolated HydA$^{\Delta EFG}$. The slightly lower activity in combination with increased Fe content relative to that obtained for the as-isolated enzyme may reflect the adventitious binding of Fe during reconstitution and/or a small percentage of partially denatured protein that resulted from the manipulation required to remove and reconstitute the iron−sulfur cluster. Nevertheless, these results clearly demonstrate that activation of HydA$^{\Delta EFG}$ by HydE, HydF, and HydG requires the presence of a preformed [4Fe-4S] cluster on HydA.

Relevance to H-Cluster Biosynthesis. In relation to the overall scheme of [FeFe]-hydrogenase maturation and H-cluster biosynthesis, these results provide significant insights into the role of HydE, HydF, and HydG maturation machinery. Because our results show that HydA$^{\Delta EFG}$ contains a redox active [4Fe-4S]$^{2+/+}$ cluster that is required for in vitro activation, logically it follows that the HydE, HydF, and HydG maturation machinery does not transfer a complete 6Fe-containing H-cluster to HydA$^{\Delta EFG}$. Moreover, HydE, HydF, and HydG maturation enzymes must be directed toward the synthesis of the 2Fe subcluster of the H-cluster or perhaps only the unique dithiolate and diatomic ligands of the 2Fe subcluster. The later hypothesis, however, seems more unlikely as CO and CN$^-$ ligands would presumably need a chemical platform of some sort (such as a 2Fe cluster) to be introduced into the maturation scheme. In light of previous work demonstrating that HydF serves as a scaffold or carrier protein which harbors an H-cluster precursor that is able to activate HydA$^{\Delta EFG}$ (*14*), the current results suggest this precursor may be some form of the 2Fe subcluster of the H-cluster.

We hypothesize that HydE and HydG function to synthesize the unique ligands on the 2Fe subcluster (CO, CN$^-$, and dithiolate ligands) using HydF as a scaffold (Figure 6). Once ligand-modified, the oxidation state of the 2Fe subcluster in its reduced active state is believed to be Fe^{I}Fe^{I} as indicated by Mössbauer and theoretical studies (*30*, *34*−*36*). We have previously proposed that HydE and/or HydG initially modifies a basic [2Fe-2S] cluster with a dithiolate ligand in chemistry analogous to sulfur−carbon bond insertion reactions by radical-SAM enzymes BioB (*37*) and LipA (*38*) in the synthesis of biotin and lipoic acid, respectively (*39*). This ligand modification should shift reactivity to the Fe atoms, setting up for further modification by addition of CO and CN$^-$ ligands. HydE and/or HydG could also be responsible for the generation CO and CN$^-$ ligands by glycine radical

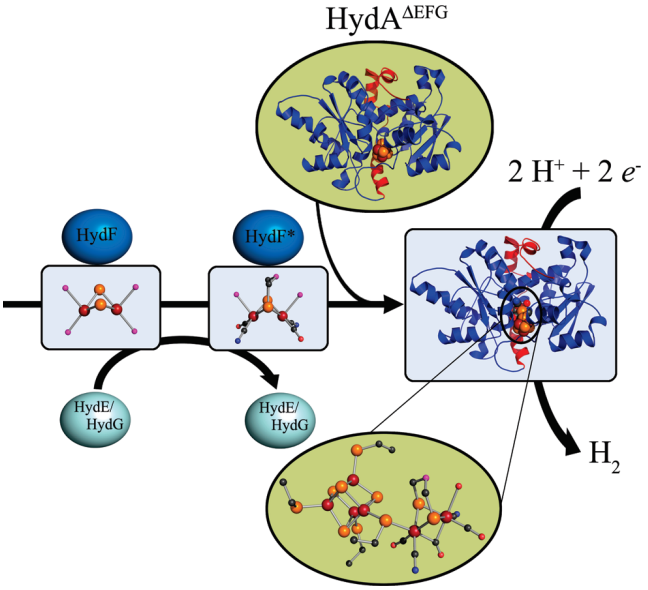

FIGURE 6: Hypothetical scheme for [FeFe]-hydrogenase maturation. In two steps, radical-SAM enzymes HydE and HydG use HydF as a scaffold to modify a basic [2Fe-2S] cluster with the addition of (1) a dithiolate ligand and (2) CO and CN$^-$ ligands. The first step is proposed to take place via a sulfur−carbon bond insertion reaction and the second step via an amino acid precursor by radical formation (*39*). The magenta atoms of the 2Fe subcluster represent hypothetical protein ligands. After assembly of the ligand-modified 2Fe subcluster, HydF* transfers it to HydA$^{\Delta EFG}$, which already houses the [4Fe-4S] subcluster of the H-cluster, completing activation of [FeFe]-hydrogenase and H-cluster biosynthesis. An atomic model of the H-cluster in activated HydA$^{\Delta EFG}$ is depicted showing the coupling of the [4Fe-4S] cubane to the 2Fe subcluster with CO, CN$^-$, and dithiolate ligands via a bridging cysteine ligand [from Protein Data Bank entry 3C8Y (*6*)]; the coloring scheme is as follows: dark red for Fe, orange for S, red for O, blue for N, dark gray for C, and magenta for an unknown atom of dithiolate ligand. Also, a water molecule is present at the distal Fe of the 2Fe subcluster in the presumed oxidized state of the H-cluster. The homology models of HydA$^{\Delta EFG}$ and HydA of *C. reinhardtii* were constructed using the homology server Phyre (*45*), and HydA from *C. reinhardtii* was threaded on HydA from *Cl. pasteurianum* (CpI) during sequence alignment. Ribbon representations of the structures were made in PyMOL (*46*) with the C-terminal domain colored red.

decomposition in a reaction analogous to those of radical-SAM enzymes [pyruvate formate lyase activating enzyme (*40*), lysine amino mutase (*41*), and ThiH (*42*)] that catalyze the formation of amino acid radicals. Alternative related proposals have been offered by Fontecave, Fontecilla-Camps, and co-workers who invoked precursors such as thiocyanate and glycine as substrates for the nonprotein ligands of the H-cluster (*43*). Regardless of these proposals, the unifying point between hypotheses is that in the final step of [FeFe]-hydrogenase maturation, HydF* transfers the ligand containing 2Fe subcluster to HydA$^{\Delta EFG}$, which already contains the [4Fe-4S] cubane of the H-cluster and is poised to accept the insertion of the 2Fe subcluster completing [FeFe]-hydrogenase activation (Figure 6). It is reasonable that HydA$^{\Delta EFG}$ can contain a [4Fe-4S] cluster without the assistance of the hydrogenase maturation proteins since *E. coli* has endogenous machinery (e.g., ISC, iron−sulfur cluster assembly system) that can easily assemble basic [4Fe-4S] clusters (*44*). Transfer of the 2Fe subcluster to HydA$^{\Delta EFG}$, already containing the [4Fe-4S] subcluster of the H-cluster, was originally proposed in a hypothesis paper regarding [FeFe]-hydogenase maturation based solely upon enzyme function and energetics (*39*).

CONCLUSIONS

We have demonstrated that $HydA^{\Delta EFG}$ from *C. reinhardtii* contains a [4Fe-4S] cluster at partial occupancy and further that the presence of this [4Fe-4S] cluster is required for in vitro activation. The presence of the iron−sulfur cluster was evidenced by chemical analysis for iron and acid-labile sulfide, as well as by spectroscopic techniques that together pointed to a $[4Fe\text{-}4S]^{2+/+}$ cluster, with an occupancy of ~40%, in the as-isolated enzyme. This [4Fe-4S] cluster-containing enzyme is capable of undergoing activation by HydE, HydF, and HydG to produce an active hydrogenase. Apo-$HydA^{\Delta EFG}$, in contrast, does not produce an active hydrogenase upon incubation with HydE, HydF, and HydG under activation conditions. These results suggested that the [4Fe-4S] cluster present in the as-isolated enzyme is required to be present on $HydA^{\Delta EFG}$ prior to activation by HydE, HydF, and HydG. Further support for this conclusion was provided by the observation that apo-$HydA^{\Delta EFG}$ reconstituted to contain a [4Fe-4S] cluster could subsequently be converted to an active hydrogenase by HydE, HydF, and HydG. Together, our results provide important new insights into the process by which HydA is matured to an active enzyme in vivo. First, a [4Fe-4S] cluster must be assembled on HydA, in a process that is presumably dependent on the housekeeping iron−sulfur cluster assembly proteins. In the second step of maturation, HydE, HydF, and HydG likely serve to synthesize, assemble, and insert the 2Fe subcluster to generate the H-cluster on HydA. Our previous results provide evidence that HydF serves as a scaffold in this process (*14*), and the radical AdoMet enzymes HydE and HydG have been proposed to catalyze the synthesis of the CO, CN^-, and dithiolate ligands to the 2Fe subcluster (*39*).

ACKNOWLEDGMENT

Portions of this research were conducted at the Stanford Synchrotron Radiation Laboratory (SSRL), a national user facility operated by Stanford University on behalf of the U.S. Department of Energy, Office of Basic Energy Sciences. The SSRL Structural Molecular Biology Program is supported by the Department of Energy, Office of Biological and Environmental Research, and by the National Institutes of Health, National Center for Research Resources, Biomedical Technology Program, and the National Institute of General Medical Sciences. We thank David Schwab and Eric Shepard of Montana State University for help in setting up the EPR instrumentation and assistance in running samples.

SUPPORTING INFORMATION AVAILABLE

EPR temperature and microwave power dependence of the $[4Fe\text{-}4S]^+$ signal (Figure S1), Mössbauer spectral components of the $[4Fe\text{-}4S]^+$ cluster signal (Figure S2), and EXAFS fit components and parameters (Figure S3 and Table S1). This material is available free of charge via the Internet at http://pubs.acs.org.

REFERENCES

1. Posewitz, M. C., King, P. W., Smolinski, S. L., Zhang, L., Seibert, M., and Ghirardi, M. L. (2004) Discovery of two novel radical S-adenosylmethionine proteins required for the assembly of an active [Fe] hydrogenase. *J. Biol. Chem. 279*, 25711–25720.
2. Adams, M. W. (1990) The structure and mechanism of iron-hydrogenases. *Biochim. Biophys. Acta 1020*, 115–145.
3. Vignais, P. M., and Billoud, B. (2007) Occurrence, classification, and biological function of hydrogenases: An overview. *Chem. Rev. 107*, 4206–4272.
4. Volbeda, A., Charon, M. H., Piras, C., Hatchikian, E. C., Frey, M., and Fontecilla-Camps, J. C. (1995) Crystal structure of the nickel-iron hydrogenase from *Desulfovibrio gigas*. *Nature 373*, 580–587
5. Peters, J. W., Lanzilotta, W. N., Lemon, B. J., and Seefeldt, L. C. (1998) X-ray crystal structure of the Fe-only hydrogenase (Cpl) from *Clostridium pasteurianum* to 1.8 angstrom resolution. *Science 282*, 1853–1858
6. Pandey, A. S., Harris, T. V., Giles, L. J., Peters, J. W., and Szilagyi, R. K. (2008) Dithiomethylether as a ligand in the hydrogenase H-cluster. *J. Am. Chem. Soc. 130*, 4533–4540
7. Nicolet, Y., Piras, C., Legrand, P., Hatchikian, C. E., and Fontecilla-Camps, J. C. (1999) *Desulfovibrio desulfuricans* iron hydrogenase: The structure shows unusual coordination to an active site Fe binuclear center. *Struct. Folding Des. 7*, 13–23
8. Nicolet, Y., de Lacey, A. L., Vernede, X., Fernandez, V. M., Hatchikian, E. C., and Fontecilla-Camps, J. C. (2001) Crystallographic and FTIR spectroscopic evidence of changes in Fe coordination upon reduction of the active site of the Fe-only hydrogenase from *Desulfovibrio desulfuricans*. *J. Am. Chem. Soc. 123*, 1596–1601
9. Bock, A., King, P. W., Blokesch, M., and Posewitz, M. C. (2006) Maturation of hydrogenases. *Adv. Microb. Physiol. 51*, 1–71
10. King, P. W., Posewitz, M. C., Ghirardi, M. L., and Seibert, M. (2006) Functional studies of [FeFe] hydrogenase maturation in an *Escherichia coli* biosynthetic system. *J. Bacteriol. 188*, 2163–2172
11. Rubach, J. K., Brazzolotto, X., Gaillard, J., and Fontecave, M. (2005) Biochemical characterization of the HydE and HydG iron-only hydrogenase maturation enzymes from *Thermatoga maritima*. *FEBS Lett. 579*, 5055–5060.
12. Brazzolotto, X., Rubach, J. K., Gaillard, J., Gambarelli, S., Atta, M., and Fontecave, M. (2006) The [Fe-Fe]-hydrogenase maturation protein HydF from *Thermotoga maritima* is a GTPase with an iron-sulfur cluster. *J. Biol. Chem. 281*, 769–774.
13. McGlynn, S. E., Ruebush, S. S., Naumov, A., Nagy, L. E., Dubini, A., King, P. W., Broderick, J. B., Posewitz, M. C., and Peters, J. W. (2007) In vitro activation of [FeFe] hydrogenase: New insights into hydrogenase maturation. *J. Biol. Inorg. Chem. 12*, 443–447.
14. McGlynn, S. E., Shepard, E. M., Winslow, M. A., Naumov, A. V., Duschene, K. S., Posewitz, M. C., Broderick, W. E., Broderick, J. B., and Peters, J. W. (2008) HydF as a scaffold protein in [FeFe] hydrogenase H-cluster biosynthesis. *FEBS Lett. 582*, 2183–2187.
15. Forestier, M., King, P., Zhang, L., Posewitz, M., Schwarzer, S., Happe, T., Ghirardi, M. L., and Seibert, M. (2003) Expression of two [Fe]-hydrogenases in *Chlamydomonas reinhardtii* under anaerobic conditions. *Eur. J. Biochem. 270*, 2750–2758.
16. Happe, T., and Kaminski, A. (2002) Differential regulation of the Fe-hydrogenase during anaerobic adaptation in the green alga *Chlamydomonas reinhardtii*. *Eur. J. Biochem. 269*, 1022–1032.
17. Winkler, M., Heil, B., Heil, B., and Happe, T. (2002) Isolation and molecular characterization of the [Fe]-hydrogenase from the unicellular green alga *Chlorella fusca*. *Biochim. Biophys. Acta 1576*, 330–334.
18. Neidhardt, F. C., Bloch, P. L., and Smith, D. F. (1974) Culture medium for enterobacteria. *J. Bacteriol. 119*, 736–747 .
19. Bradford, M. M. (1976) A rapid and sensitive method for the quantitation of microgram quantities of protein utilizing the principle of protein-dye binding. *Anal. Biochem. 72*, 248–254.
20. Fish, W. W. (1988) Rapid colorimetric micromethod for the quantitation of complexed iron in biological samples. *Methods Enzymol. 158*, 357–364.
21. Beinert, H. (1983) Semi-micro methods for analysis of labile sulfide and of labile sulfide plus sulfane sulfur in unusually stable iron-sulfur proteins. *Anal. Biochem. 131*, 373–378.
22. Broderick, J. B., Henshaw, T. F., Cheek, J., Wojtuszewski, K., Smith, S. R., Trojan, M. R., McGhan, R. M., Kopf, A., Kibbey, M., and Broderick, W. E. (2000) Pyruvate formate-lyase-activating enzyme: Strictly anaerobic isolation yields active enzyme containing a $[3Fe\text{-}4S]^+$ cluster. *Biochem. Biophys. Res. Commun. 269*, 451–456.
23. Ravel, B., and Newville, M. (2005) *ATHENA, ARTEMIS, HEPHAESTUS*: Data analysis for X-ray absorption spectroscopy using *IFEFFIT*. *J. Synchrotron Radiat. 12*, 537–541
24. Rehr, J. J., and Albers, R. C. (2000) Theoretical approaches to X-ray absorption fine structure. *Rev. Mod. Phys. 72*, 621
25. Rao, P. V., and Holm, R. H. (2004) Synthetic analogues of the active sites of iron-sulfur proteins. *Chem. Rev. 104*, 527–559
26. Ugulava, N. B., Gibney, B. R., and Jarrett, J. T. (2001) Biotin synthase contains two distinct iron-sulfur cluster binding sites: Chemical and spectroelectrochemical analysis of iron-sulfur cluster interconversions. *Biochemistry 40*, 8343–8351.

27. Johnson, M. K. (1994) Iron-sulfur proteins. In Encyclopedia of inorganic chemistry (King, R. B., Ed.) pp 1896−1914, John Wiley & Sons Ltd., West Sussex, England.
28. Rupp, H., Rao, K. K., Hall, D. O., and Cammack, R. (1978) Electron spin relaxation of iron-sulphur proteins studied by microwave power saturation. *Biochim. Biophys. Acta 537*, 255–260.
29. Middleton, P., Dickson, D. P., Johnson, C. E., and Rush, J. D. (1978) Interpretation of the Mössbauer spectra of the four-iron ferredoxin from *Bacillus stearothermophilus*. *Eur. J. Biochem. 88*, 135–141.
30. Pereira, A. S., Tavares, P., Moura, I., Moura, J. J., and Huynh, B. H. (2001) Mössbauer characterization of the iron-sulfur clusters in *Desulfovibrio vulgaris* hydrogenase. *J. Am. Chem. Soc. 123*, 2771–2782.
31. Teo, B.-K., Shulman, R. G., Brown, G. S., and Meixner, A. E. (1979) EXAFS studies of proteins and model compounds containing dimeric and tetrameric iron-sulfur clusters. *J. Am. Chem. Soc. 101*, 5624–5631.
32. Beinert, H., Emptage, M. H., Dreyer, J. L., Scott, R. A., Hahn, J. E., Hodgson, K. O., and Thomson, A. J. (1983) Iron-sulfur stoichiometry and structure of iron-sulfur clusters in three-iron proteins: Evidence for [3Fe-4S] clusters. *Proc. Natl. Acad. Sci. U.S.A. 80*, 393–396.
33. Musgrave, K. B., Angove, H. C., Burgess, B. K., Hedman, B., and Hodgson, K. O. (1998) All-ferrous titanium(III) citrate reduced Fe protein of nitrogenase: An XAS study of electronic and metrical structure. *J. Am. Chem. Soc. 120*, 5325–5326.
34. Popescu, C. V., and Munck, E. (1999) Electronic structure of the H cluster in [Fe]-hydrogenases. *J. Am. Chem. Soc. 121*, 7877–7884.
35. Cao, Z., and Hall, M. B. (2001) Modeling the active sites in metalloenzymes. 3. Density functional calculations on models for [Fe]-hydrogenase: Structures and vibrational frequencies of the observed redox forms and the reaction mechanism at the diiron active center. *J. Am. Chem. Soc. 123*, 3734–3742.
36. Liu, Z. P., and Hu, P. (2002) A density functional theory study on the active center of Fe-only hydrogenase: Characterization and electronic structure of the redox states. *J. Am. Chem. Soc. 124*, 5175–5182.
37. Duin, E. C., Lafferty, M. E., Crouse, B. R., Allen, R. M., Sanyal, I., Flint, D. H., and Johnson, M. K. (1997) [2Fe-2S] to [4Fe-4S] cluster conversion in *Escherichia coli* biotin synthase. *Biochemistry 36*, 11811–11820.
38. Miller, J. R., Busby, R. W., Jordan, S. W., Cheek, J., Henshaw, T. F., Ashley, G. W., Broderick, J. B., Cronan, J. E.Jr., and Marletta, M. A. (2000) *Escherichia coli* LipA is a lipoyl synthase: In vitro biosynthesis of lipoylated pyruvate dehydrogenase complex from octanoyl-acyl carrier protein. *Biochemistry 39*, 15166–15178.
39. Peters, J. W., Szilagyi, R. K., Naumov, A., and Douglas, T. (2006) A radical solution for the biosynthesis of the H-cluster of hydrogenase. *FEBS Lett. 580*, 363–367.
40. Kulzer, R., Pils, T., Kappl, R., Huttermann, J., and Knappe, J. (1998) Reconstitution and characterization of the polynuclear iron-sulfur cluster in pyruvate formate-lyase-activating enzyme. Molecular properties of the holoenzyme form. *J. Biol. Chem. 273*, 4897–4903.
41. Frey, P. A. (2001) Radical mechanisms of enzymatic catalysis. *Annu. Rev. Biochem. 70*, 121–148.
42. Leonardi, R., Fairhurst, S. A., Kriek, M., Lowe, D. J., and Roach, P. L. (2003) Thiamine biosynthesis in *Escherichia coli*: isolation and initial characterisation of the ThiGH complex. *FEBS Lett. 539*, 95–99.
43. Pilet, E., Nicolet, Y., Mathevon, C., Douki, T., Fontecilla-Camps, J. C., and Fontecave, M. (2009) The role of the maturase HydG in [FeFe]-hydrogenase active site synthesis and assembly. *FEBS Lett. 583*, 506–511.
44. Barras, F., Loiseau, L., and Py, B. (2005) How *Escherichia coli* and *Saccharomyces cerevisiae* build Fe/S proteins. *Adv. Microb. Physiol. 50*, 41–101.
45. Bennett-Lovsey, R. M., Herbert, A. D., Sternberg, M. J., and Kelley, L. A. (2008) Exploring the extremes of sequence/structure space with ensemble fold recognition in the program Phyre. *Proteins 70*, 611–625.
46. DeLano, W. L. (2002) The PyMol molecular graphics system , DeLano Scientific, Palo Alto, CA.